Keynote Lecture: Application of advanced numerical analysis in geotechnical engineering design

Lidija Zdravković
Imperial College London, London, United Kingdom. E-mail: l.zdravkovic@imperial.ac.uk

David M. Potts
Imperial College London, London, United Kingdom. E-mail: d.potts@imperial.ac.uk

Keywords: numerical analysis, constitutive models, boundary conditions

ABSTRACT: Geotechnical analysis is an integral part of the geotechnical design process. It is performed with the aim of assessing the stability and serviceability of geotechnical structures and their interaction with the natural and built environment. The complexities of many geotechnical problems and requirements for long-term design solutions increasingly require the use of advanced numerical analysis. This paper explores the application of advanced numerical tools in the lifecycle assessment of infrastructure slopes in stiff clays and of earthfill infrastructure embankments.

1. INTRODUCTION

The complexities of many contemporary geotechnical problems, such as long-term infrastructure resilience, sustainable construction, lasting solutions for nuclear waste disposal, exploration of new forms of renewable energy such as geothermal and wind, all potentially compounded by the anticipated effects of climate change, can often be tackled only by employing advanced numerical analysis. At present, the finite element (FE) method is the most widespread computational tool for sophisticated geotechnical calculations and this paper focuses on advanced FE analysis.

The main components of geotechnical design to be considered in a numerical analysis could be grouped into assessments of problem geometry, ground conditions and design requirements (Fig. 1), that all need to be idealised in a realistic manner as input to the numerical model. The problem geometry needs to be discretised into a FE mesh using appropriate element types to present both the soil and structural components such as walls, tunnel linings, or anchors, and any interfaces between different materials. The available laboratory and field data from ground investigation has to be integrated to both characterise the soil behaviour and establish the initial ground conditions (in terms of stresses, pore pressures, void ratio / relative density, temperature, or degree of saturation, depending on the soil type and type of analysis to be performed). This step of idealisation has to be consistent with a selected soil constitutive model and the level of model sophistication usually depends on the available experimental data. Finally, designing for the processes involved in a given problem, such as excavation, construction, loading, dewatering, change in temperature, or rainfall infiltration, requires application of appropriate boundary conditions. The competency of numerical analysis strongly depends on all steps of idealisation.

This paper explores the application of advanced FE analysis using examples of infrastructure slopes and embankments. It draws on extensive experience in computational geomechanics at Imperial College London, comprising the bespoke development of the Imperial College Finite Element Program (ICFEP, Potts & Zdravković, 1999, 2001) and its application in research projects and practical applications. ICFEP employs a modified Newton-

P. Duc Long and N. T. Dung (eds.) et al., *Geotechnics for Sustainable Infrastructure Development*, Lecture Notes in Civil Engineering 62,
https://doi.org/10.1007/978-981-15-2184-3_132

Raphson non-linear solver, with an error-controlled sub-stepping stress-point algorithm.

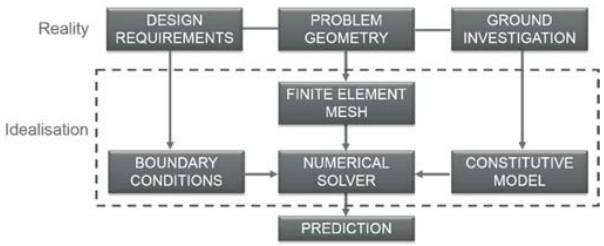

Figure 1. Numerical idealisation

2. CUT SLOPES IN STIFF PLASTIC CLAYS

One of the main characteristic of stiff plastic clays is their brittle stress-strain behaviour, depicted schematically in Fig. 2, mobilising the peak stress early in shearing, followed by softening upon further increase in shear strain and stabilisation at much lower residual stresses. Early numerical studies at Imperial College in 1980s and '90s identified and quantified this behaviour as the main reason behind delayed collapses of many infrastructure slopes in stiff plastic clays in the UK, some failing even 100 years after their first excavation (Potts et al., 1990, 1997; Dounias et al., 1996; Kovacevic et al., 2007).

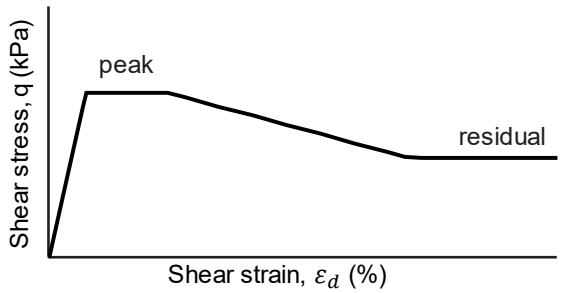

Figure 2. Strain-softening behaviour

2.1 Ultimate Limit States (ULS)

A principal aspect of design and re-design of cut slopes has been their stability in the long-term. Consequently, the constitutive model has to be capable of simulating the behaviour depicted in Fig. 2. Equally, the FE analysis has to be hydro-mechanically coupled in terms of the governing equations, in order to capture the transient consolidation in the soil after slope excavation.

2.1.1 Constitutive model

The work of Kovacevic (1994) and Potts et al. (1997) focussed on slopes in London clay, which is an overconsolidated medium-plastic clay (*PI*= 37%). The adopted constitutive model was a strain-softening Mohr-Coulomb model. The strength parameters c' (effective cohesion) and ϕ' (angle of shearing resistance) were assigned the peak values of 7 kPa and 20°, respectively, and residual values of 2 kPa and 13°, respectively. The peak and residual strengths were mobilised at 5% and 20% of plastic deviatoric strain (ε_d^p), respectively. The angle of dilation was set to 0°.

The permeability, k, of London clay was modelled as isotropic and stress-level dependent (Vaughan, 1994), according to Eq. (1):

$$k = k_0 \cdot \exp^{-b \cdot p'} \tag{1}$$

where $k_0 = 5 \times 10^{-10}$ m/s, b=0.003m^2/kN is a model parameter and p' is the mean effective stress.

2.1.2 Boundary conditions

The excavation of the slope, simulated over a period of 3 months, is practically undrained due to the low permeability of London clay. This process causes a depression of the initial phreatic surface in the soil (located at 1.0 m depth below the ground surface), creating suctions (negative pore water pressures) at the end of excavation, as depicted in Fig. 3. In the transient post-excavation stage the phreatic surface changes to reach a hydraulic equilibrium (steady state) with the hydraulic boundary condition prescribed on the excavated surface. It is during this stage that the slope may fail before reaching the steady state, as suctions gradually reduce, thus reducing effective stresses in the slope and causing non-uniform mobilisation of shear strength which promotes the propagation of the potential rupture surface.

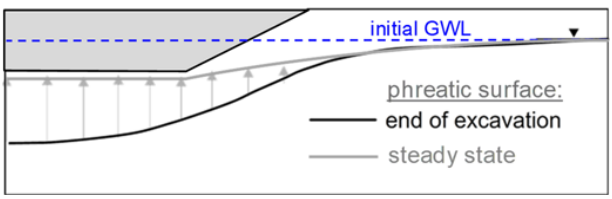

Figure 3. Simulation of slope excavation

The hydraulic boundary condition applied to the excavated slope surface and to the remaining ground surface is that of a constant pore fluid pressure equal to 10 kPa of suction (as shown in a typical FE mesh in Fig. 4). This hydraulic boundary condition is derived from the piezometric measurements of pore water pressures (Fig. 5) in natural, cut and embankment slopes in clays, collected in central and southern England over several years (Walbancke,

1976; Vaughan, 1994). The figure shows maximum winter and minimum summer measurements, indicating the extent of seasonal variations to 4.0 m depth below ground surface. The probable average surface value of pore water pressure may be derived by extrapolating the steady conditions from below 4.0 m depth to the ground surface (as shown in Fig. 5), giving a value of 10 kPa suction (i.e. -1.0 m head). The remaining boundaries of the soil domain are impermeable, allowing no flow of water across.

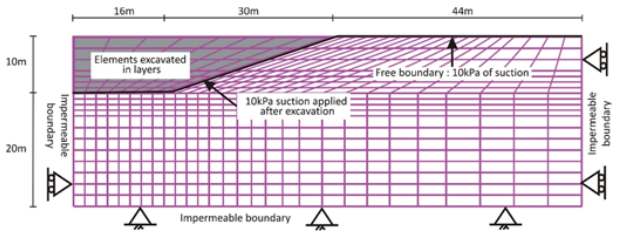

Figure 4. Typical FE mesh for cut slope

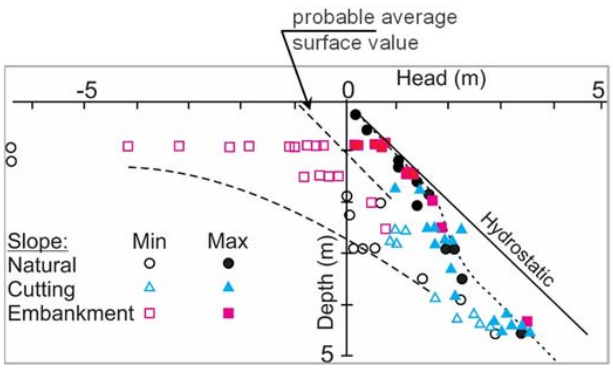

Figure 5. Pore pressure measurements in UK slopes (after Vaughan, 1994)

2.1.3 *Results*

The study of London clay cut slopes by Kovacevic (1994) and Potts et al. (1997) demonstrated the transient progression of the rupture surface in typical 1:3 gradient slopes (vertical to horizontal) and enabled quantification of time over which the slopes remain stable. Fig. 6 shows that a 10 m deep slope fails 14.5 years after excavation, for the soil properties and boundary conditions given above.

Further parametric studies were conducted varying the initial ground conditions (i.e. the earth pressure coefficient, K_0), the surface hydraulic boundary conditions (i.e. the magnitude of surface suction) and slope inclination. The results are summarised in Fig. 7 in terms of the magnitude of the mid-slope horizontal movement versus the time to failure.

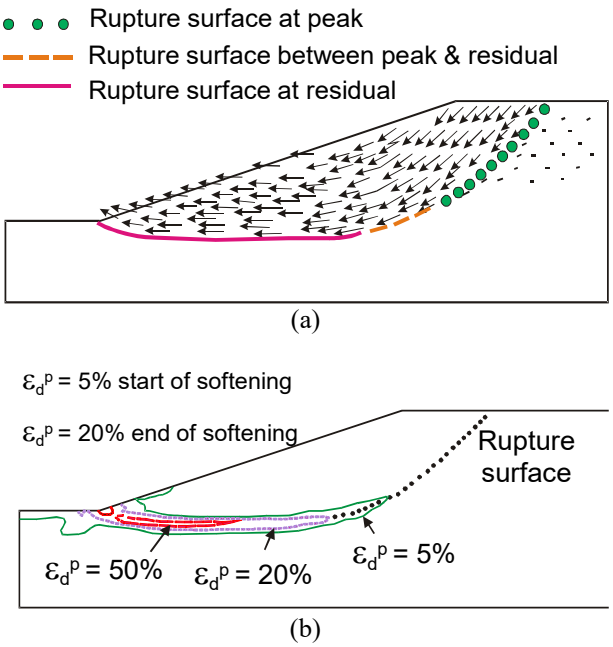

Figure 6. Progression of the rupture surface at 14.5 years after excavation: (a) vectors of ground movements and (b) deviatoric plastic strains in the rupture surface (after Potts et al., 1997)

2.2 *Further considerations*

2.2.1 *Mesh dependency*

It is widely recognised that the FE modelling of a strain softening material is challenging, as achieving the appropriate rate of softening for a given soil, as observed in laboratory experiments, is mesh-dependent. This is explained by the fact that the plastic shear strain developed along a rupture surface (or a shear band) is calculated from the displacement components computed at the nodes of the elements in the immediate vicinity (the so-called 'local' approach), influencing both the direction of the shear band propagation and its thickness (Galavi & Schweiger, 2010). Consequently, there is a high dependency of numerical predictions on the size of the finite elements in the mesh (Vardoulakis & Sulem, 1995).

To improve the modelling of strain-softening materials a number of techniques has been proposed in the literature. Those that provide more rigorous approximations of the shear zone are the Cosserat concepts (Bazant & Jirasek, 2002), gradient plasticity (e.g. Zervos et al., 2001) and non-local approaches (e.g. Vermeer & Brinkgrave, 1994; Galavi & Schweiger, 2010).

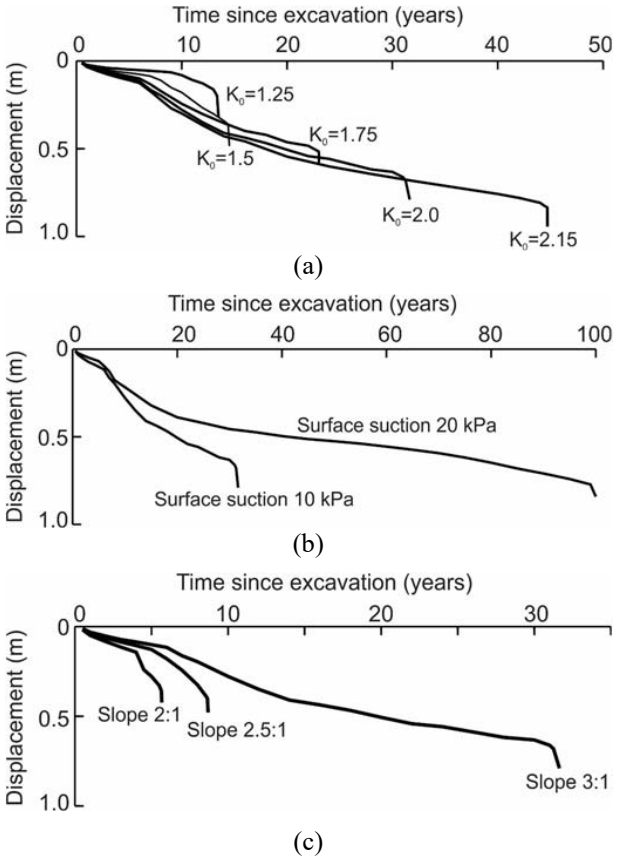

Figure 7. Effect of (a) K_0; (b) surface suction and (c) slope inclination on time to failure (after Potts et al., 1997)

The studies of Kovacevic (1994) and Potts et al. (1997), discussed in Section 2.1, were performed with the local strain approach and therefore addressed with great care the element size in their FE meshes. In effect, the softening rate and the strain limits of the softening path were derived from the comparison of experimental data with simple shear FE simulations, such that the displacements for the limits of softening from the latter were related to the element sizes in the mesh used for the analysed cut slope. More recently, Summersgill (2015) and Summersgill et al. (2017) investigated different non-local strain regularisation techniques and found that of Galavi & Schweiger (2010) to be superior to others examined. This technique was implemented in ICFEP, affecting both the formulation of the strain softening Mohr-Coulomb model and of the numerical solver. The essence of the non-local approach is that the plastic shear strain in the shear band is calculated not only from the displacements at nodes in the immediate vicinity, but from a larger area around the point at which the strain calculation is performed. Two regularisation parameters become an input to the constitutive model: 'defined length' (DL), which influences the distribution of the weighting functions for all contributing nodes; and the 'radius of influence' (RI) that defines the size of the area around the calculation point from which the strains will be included in the non-local strain calculation.

Using this approach Summersgill et al. (2017) extended the study of cut slopes in London clay, adopting the same hydro-mechanical properties of the soil as in Section 2.1, the geometry of slope given in Fig. 4 and additional parameters *DL*=2.1 m and *RI*= 6.3 m (=3 x *DL*). Creating a number of different meshes, with different element sizes that were not designed to necessarily match the strain softening rate observed experimentally (as was ensured in Potts et al. 1997), the results presented in Fig. 8, in terms of the magnitude of the mid-slope horizontal movement versus the time to failure, show that the latter varies from about 15 to over 250 years post-slope excavation, demonstrating very clearly the potential inaccuracies of the standard local strain FE calculations in strain softening soils. Application of the non-local regularisation method significantly reduced this range to 38 to 85 years, although still leaving some uncertainty in the results.

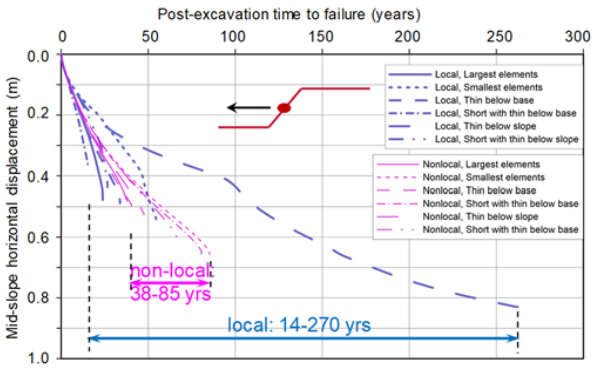

Figure 8. Effect of the local and non-local strain models on the predicted time to failure of a cut slope (after Summersgill et al., 2017)

The Summersgill et al. (2017) study also examined the effect of the strain regularisation approach on the predicted factor of safety in the slope. The analyses again used different meshes (in terms of the number and size of elements) for the same slope (shown in Fig. 4), applying, after the slope excavation, the strength-reduction technique developed by Potts & Zdravkovic (2012) and implemented in ICFEP. The latter approach applies to any constitutive model and its formulation introduces changes to both constitutive and governing FE equations. In the case of the Mohr-

Coulomb model, the characteristic values (derived from available soil data) of both c' and ϕ' are gradually reduced by an increasing factor, F, until the slope failure is fully mobilised, at which point the final value of F becomes the factor of safety, F_s:

$$c' = \frac{c'_{ch}}{F_s} \tag{2}$$

$$\phi' = \tan^{-1}\left(\frac{\tan\phi'_{ch}}{F_s}\right) \tag{3}$$

Fig. 9 compares the magnitudes of F_s predicted from local and non-local strain regularisation models, applied to a selection of FE meshes for the same slope. The range of values from the local model is 1.37 to 1.51, while a much narrower range of 1.41 to 1.44 is predicted by the non-local model, demonstrating again the importance of the latter development when analysing strain softening soils.

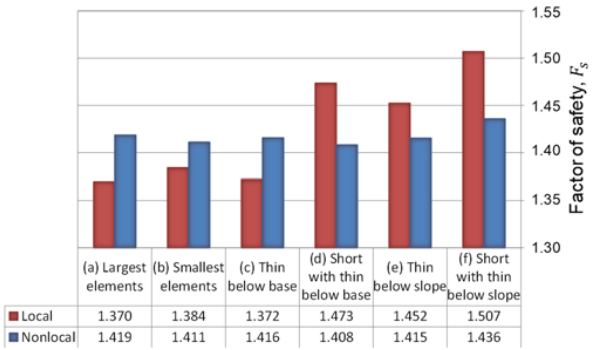

Figure 9. Predicted factor of safety from local and non-local strain models (after Summersgill et al., 2017)

2.2.2 *Strain-rate effects*

Recent experimental research at Imperial College Geotechnical Laboratory involved detailed comparative study of the stiffness and strength characteristics of stiff clays which underlain the southern part of the UK. In addition to London clay (Gasparre, 2005; Hight et al., 2007), three geologically older clays, Gault, Kimmeridge and Oxford, were also investigated (Brosse, 2012; Hosseini Kamal, 2012; Hosseini Kamal et al., 2014; Brosse et al. 2017). The gathered experimental data has been valuable in examining the behaviour of cut slopes in these clays, considering the likelihood of the UK's high speed rail route, currently in the planning, passing through these materials.

In terms of their stress-strain behaviour, Oxford clay exhibits significantly more brittle behaviour than either of the three other clays. This aspect of behaviour was examined in the numerical study of Zdravkovic et al. 2019 and Ho 2019, which further investigated the stability of cut slopes in stiff plastic clays. In the first instance, the geometry of the slope was varied for the ground conditions corresponding to London clay, derived by Kovacevic at al. 2007 for the analyses of temporary slopes excavated as part of the ground works during the construction of Heathrow Terminal 5. The same strain softening Mohr-Coulomb model was adopted in the new study, employing the non-local strain regularisation. The strength parameters in this case were 8 kPa and 25° for the peak values of c' and ϕ', respectively, and 2 kPa and 13° for the residual strengths, respectively, with the limits of softening being 2% and 15% of the deviatoric plastic strain. Additionally, the non-liner small strain overlay model IC3GS of Taborda & Zdravkovic (2012) and Taborda et al. (2016), which allows an independent control of the shear, G, and bulk, K, moduli and their dependency on stress, p', and strain (deviatoric, ε_d, and volumetric, ε_{vol}, respectively) levels, was coupled with the plastic model to capture more accurately the small strain response of London clay. The hydraulic boundary conditions were the same as described in Section 2.1, maintaining 10 kPa suction on the excavated slope surface. The slope heights of 5, 10, 15 and 20 metres and inclinations of 1:4, 1:3 and 1:2.5 were examined. The FE results revealed that slopes with 1:3 inclination or flatter (1:4) and up to 10 m high were stable over the period of 120 years, considered to be their design life. As an example, the contours of deviatoric plastic strains in Fig. 10, for the 1:3, 10 m high slope and at post-excavation time of 120 years, show that the shear surface started to develop, which took place over the first 10 years after slope excavation, but then remained stable to 120 years.

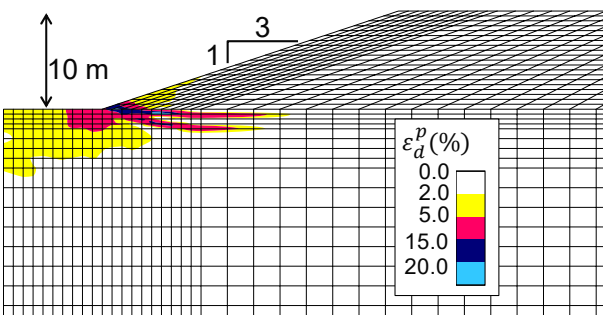

Figure 10. Contours of deviatoric plastic strains at 120 years post excavation; stable shear surface

These parametric analyses further revealed that steeper slopes (1:2.5) were stable only if 5 m high,

while even flatter 1:4 slopes, but 15 or 20 m high, failed within 10 to 20 years post-excavation.

Additional parametric analyses were performed to investigate the effect of the strain softening rate, applying a faster rate in the constitutive model (similar to that of Oxford clay). The same peak and residual strength parameters as for London clay were adopted, but the limits of softening were prescribed to be 2% and 8.5% of the deviatoric plastic strain (compared to the above 2% and 15%). The contours of deviatoric plastic strains in Fig. 11, for the previously stable 1:3, 10 m high slope, show a fully developed shear surface, and hence failure of the slope, 21 years post-excavation.

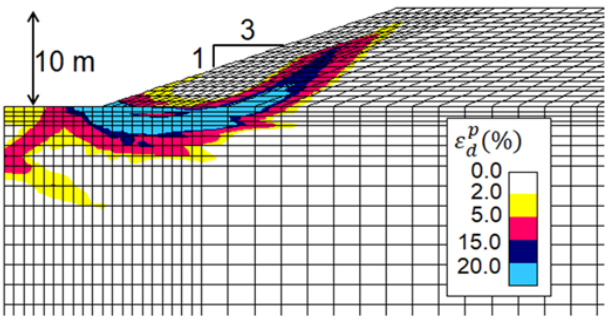

Figure 11. Contours of deviatoric plastic strain at failure, 21 years post-excavation

2.2.3 *Serviceability limit states (SLS)*

While the stability was a key design requirement for cut slopes studied in the 1990s, current design requirements are additionally concerned with the magnitudes of heave across the base of the excavation. This is led by new technologies of railway track placements which are sensitive to excessive ground movements, hence having tight tolerances. From the slope geometries investigated in Section 2.2.2 for their stability, the 5 and 10 m high slopes in London clay with inclinations 1:3 and 1:4, which were shown to remain stable over their design life, are also examined for the magnitudes of base heave post-slope excavation.

The magnitudes of ground movements during excavation, which is predominantly undrained due to the low permeability of London clay, are controlled by the shear modulus, *G*, in the soil. However, movements in the transient post-excavation stages are controlled principally by the bulk modulus, *K*, which is a property not always readily interpreted from ground investigations, and by soil permeability, which is equally difficult to estimate accurately from laboratory or field measurements. The study of Zdravkovic et al. 2019 demonstrated a significant level of sensitivity of the predicted magnitude of base have with respect to the bulk modulus and permeability interpreted from available experimental data.

Fig. 12 presents the experimental data of the normalised secant bulk modulus, K/p', degradation with volumetric strain, interpreted from the isotropic recompression stages of London clay triaxial samples before they were subjected to shearing (Gasparre, 2005). The black line plotted within the scatter of experimental data represents the bulk modulus based on the Kovacevic et al. 2007 calibration and reproduced by the IC3GS model, having $(K/p')_{\min} = 40$. As the non-linear small strain part of the curve (up to 0.1% volumetric strain) mobilises reasonably quickly post-excavation, the magnitude of the long-term heave is essentially controlled by the magnitude of the bulk modulus in the medium to large volumetric strain range (over 0.1%). To demonstrate this, two additional curves in Fig. 12 were derived to coincide with the small strain part of the black line, but limiting the $(K/p')_{\min}$ to either 20 or 60 in the medium to large strain range. All three curves plot within the scatter of experimental data.

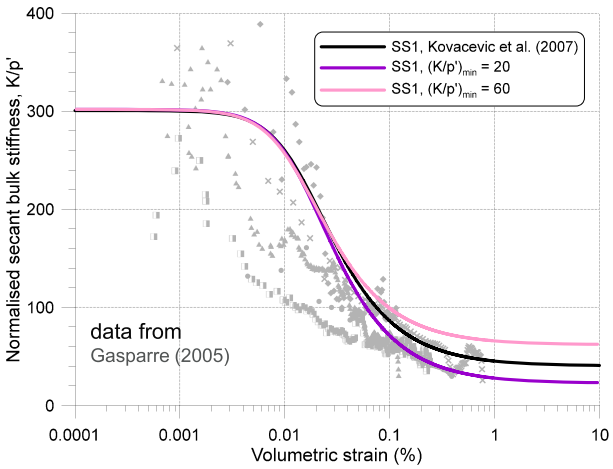

Figure 12. Calibrated bulk modulus degradation

Fig. 13 shows evolutions of the post-excavation base heave for a 1:3, 10 m high slope in London clay. The three curves result from the three FE analyses which differ only in the adopted bulk modulus degradation curve, shown in Fig. 12. These results clearly demonstrate the significant effect of the bulk modulus calibration in the medium to large strain range, as the total magnitude of heave ranges from 110 to 215 mm, obtained for the smallest and largest value of $(K/p')_{\min}$, respectively. The time

to achieving full heave is also significantly shorter for the higher bulk modulus (21 years) compared to 51 years for the smallest bulk modulus. Even if a pause period of 1 year is allowed before track placement, only a fraction of the heave would have mobilised in this slope, meaning that a significant amount of heave is yet to develop during the operational stage of the track (52 to 138 mm range for the bulk modulus curves in Fig. 12).

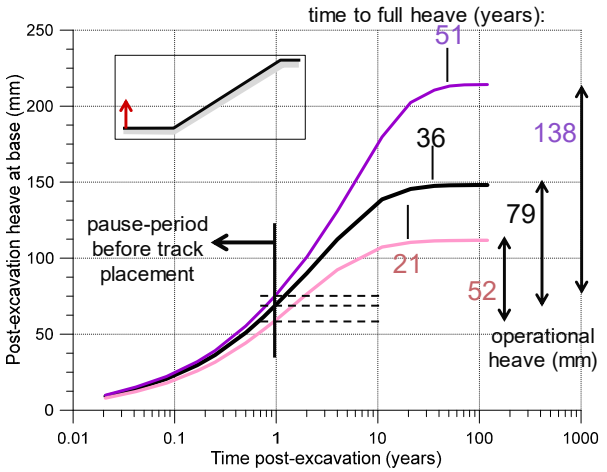

Figure 13. Post-excavation heave as a function of bulk modulus

Similar uncertainties in the predictions of base heave are caused by uncertainties in the interpretations of soil permeability. The data from Hight et al. (2003), plotted in Fig. 14, show the scatter of permeability measurements in London clay. Fitted through the data are profiles of permeability according to the permeability model in Eq. (1). The black line is the average profile from the Kovacevic et al. (2007) study, which was used in all the above analyses where the bulk modulus curve was varied. The two additional permeability profiles in Fig. 14 are fitted through the lower and higher range of permeability data, while the bulk modulus curve associated with all three profiles is the same as that of Kovacevic et al. (2007) (black line in Fig. 12). The results from these three analyses showed that the magnitude of the total post-excavation heave is the same (about 150 mm, as shown in Fig. 13), as this is controlled by the bulk modulus. The permeability, however, controls the rate of evolution of heave. For the profile of higher permeability full heave was mobilised 11 years post-excavation, while the profile of lower permeability showed stable heave almost at 120 years post-excavation, meaning that the base of the track is deforming throughout its design life. The result from the whole serviceability study showed a reasonably small operational heave (10 to 20 mm) only for the 5 m high slopes with 1:3 and 1:4 sides. The range of operational heave for 1:3 and 1:4 10 m high slopes is 50 to 150 mm. This would be much large larger for higher slopes; they were however showed earlier to be unstable in the long term.

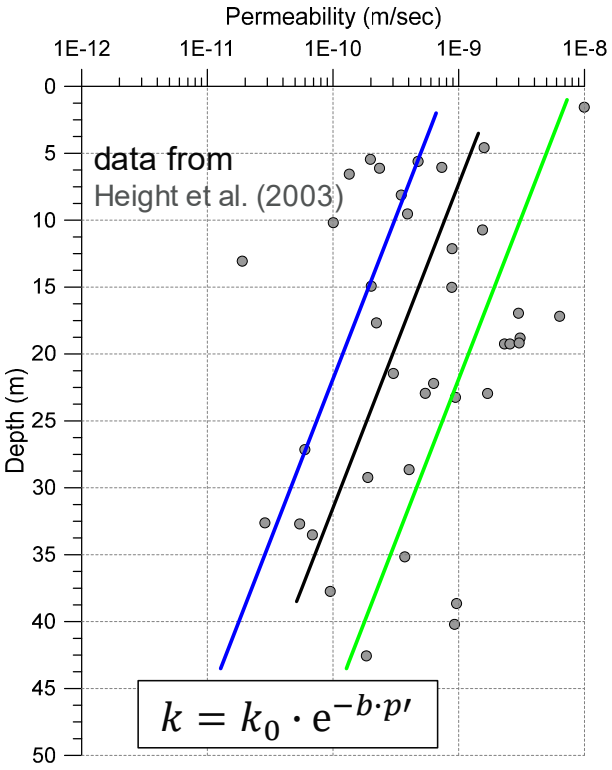

Figure 14. Calibrated permeability profiles

The results on stability (considering strain softening rate) and serviceability (considering bulk modulus and permeability) of cut slopes discussed in this section have significant implications for the economy of the design of cut slopes in stiff overconsolidated clays. In most cases the results indicate the necessity for implementation of mitigation measures to either improve the stability or reduce the level of heave. The analysis also highlights the facets of soil behaviour that need to be more accurately characterised by site investigations in order to reduce the range of uncertainty in experimental data.

3. EARTHFILL EMBANKMENTS

Similar to infrastructure slopes, the design and re-design of infrastructure embankments increasingly requires the whole life-cycle assessment of their stability and serviceability. The remit of such assessment is becoming more complicated due to the necessity to bring into calculations more realistic representation of, in particular, hydraulic boundary

conditions on the exposed surfaces of slopes and embankments. Increasingly changing weather patterns around the world, including the UK, are making earth structures more prone to rainfall-induced instabilities (e.g. Fig. 15 from UK) due to an increased frequency and/or intensity of extreme weather conditions (both rainfalls and droughts). Vegetation management on cut slopes and embankment slopes is seen as a measure of improving their stability and serviceability. In the light of a life-cycle assessment, the effects of climate change on the evolving weather patterns must also be taken into consideration, making an advanced numerical analysis even more complex. The FE analysis of earth embankments is also challenged by the fact that the embankment body is unsaturated in its initial state, hence requiring the governing equations and constitutive models that can account for the behaviour of unsaturated soils.

Figure 15. Stonegate slip on the London to Exeter line, UK, in February 2014 (photo: @networkrail)

3.1 Hydraulic boundary conditions

The studies on cut slopes presented in Section 2 adopted a hydraulic boundary condition of constant pore pressure (or suction) on the excavated surface of the slope and on the remaining ground surface. As explained, this was an average surface pressure derived from seasonal variations of pore pressure measured over a number of years, hence representing a stable boundary condition. However, application of such a boundary condition would not be able to predict the type of failure shown in Fig. 15, which is induced by water infiltration from the surface, rather than by equilibration of pore pressures in the ground. In such a case the FE analysis needs to simulate realistic rainfall records, as shown in the example in Fig. 16, together with appropriate modelling of vegetation that takes water out of the ground, contributing to complex mechanisms of soil-plant-atmosphere interaction (SPAI). Fig. 16 is an example of a rainfall record from a particular measurement station in the south-east England, which shows a steady pattern up to recent years, and two significant peaks with over 80 mm daily rainfall that correspond to storms in 2013 and 2014.

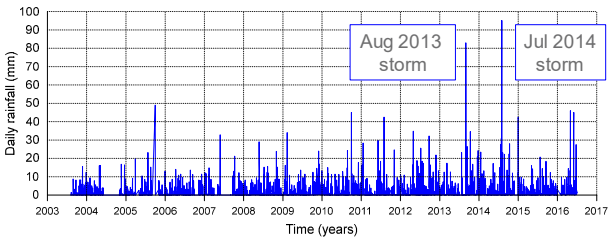

Figure 16. Example of a rainfall record (after Guo, 2020)

Zdravkovic et al. (2018) and Tsimapousi et al. (2017c) discuss the necessary ingredients of the FE analysis, as developed and implemented in ICFEP, to realistically reproduce the given SPAI conditions. These include the modelling of permeability and application of hydraulic boundary conditions such as precipitation and evapotranspiration.

3.1.1 Precipitation

This is a dual boundary condition that prescribes either the magnitude of flow rate or the magnitude of pore water pressure along a boundary (Potts and Zdravkovic, 1999). In the case of modelling rainfall, if the soil has sufficient permeability and/or the rainfall intensity is small, the soil may be able to absorb the water and therefore a flow boundary condition is appropriate, prescribing the flow rate, q_{nb}, over the boundary. Otherwise, if the soil is less permeable and/or rainfall intensity is high, the soil may not be able to absorb all of the water, with ponding on the surface or running off the excess. In this case a pore pressure boundary condition would be applicable, prescribing the appropriate magnitude of the pore fluid pressure, p_{fb}, on the boundary.

Clearly, depending on the geometry of the problem and on how the permeability changes during the analysis, it is impossible to make in advance the appropriate choice between these two boundary conditions for each increment of the analysis. The precipitation boundary condition is therefore needed as it enables an automatic decision on the boundary condition to be made over each

increment. Namely, at the beginning of each increment the pore fluid pressure at boundary nodes is compared to p_{fb} and if found to be more tensile, then an infiltration boundary condition is activated, with the flow rate equal to q_{nb}. Conversely, if found to be more compressive, a pore fluid pressure equal to p_{fb} is prescribed along the boundary. As conditions may change during an increment of the analysis, hence needing a switch from the boundary condition detected at the beginning of that increment, an automatic incrementation (AI) algorithm is required.

The AI algorithm available in ICFEP is based on the work of Abbo and Sloan (1996) and Sheng and Sloan (2001), for stress-strain behavior in nonlinear finite element analysis. Its further development, to operate in conjunction with the precipitation boundary condition, is detailed in Smith (2003) and Smith et al. (2008). The purpose of the AI algorithm is to break down the size of the initial increment to smaller sub-increments in order to apply an appropriate precipitation boundary condition (i.e. flow rate or pore fluid pressure) as it changes over the increment.

3.1.2 Evapotranspiration

The amount of water uptake from a depth below the ground surface is governed by the root depth and density, permeability of the soil-root system and the availability of water. In the actual finite element analysis this uptake of water is incorporated in the sink term of the continuity equation (see Zdravkovic et al., 2018) and in ICFEP it is simulated with the root water uptake model (RWUM) developed by Nyambayo and Potts (2010).

The RWUM requires the potential evapotranspiration rate to be prescribed for each increment of the analysis. The sink term, $S_{\max}$, is assumed to vary linearly with depth, *r*, below the ground surface, as depicted in Fig. 17a, and is defined as:

$$S_{\max} = \frac{2T_p}{r_{\max}}\left(1 - \frac{r}{r_{\max}}\right) \tag{4}$$

where $r_{\max}$ is the maximum root depth. This is an input parameter for this boundary condition and reflects the limit depth below which the root water uptake is zero. Eq. (4) presents how much water could potentially be extracted if the supply of water in the ground was unlimited. However, the supply of soil moisture is normally not unlimited and therefore the actual evapotranspiration is smaller than the potential value. To calculate the actual evapotranspiration, the sink term $S_{\max}$ is multiplied by a suction-dependent parameter α, according to Feddes at al. (1978), which is assumed to vary with suction, as depicted in Fig. 17b. Values of suctions *S1* to *S4* are input parameters. At suctions outside the two limits, *S1* and *S4*, the root water uptake is assumed to be zero. The former relates to water-logged conditions in the soil when roots are unable to function, whereas the latter relates to the permanent wilting point.

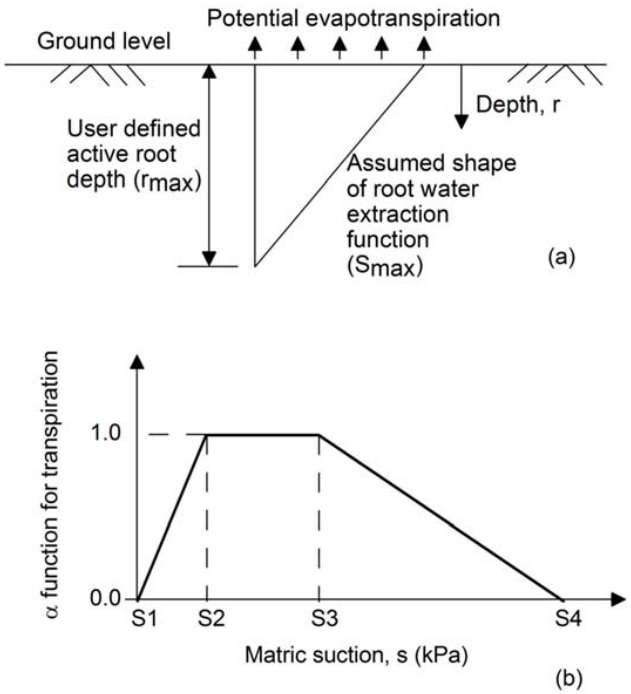

Figure 17. (a) Watere extraction function when $\alpha = 1$; (b) variation of the α -function with suction

3.2 Permeability

Realistic modelling of soil permeability is particularly pertinent in problems involving atmospheric effects of rainfall infiltration and evapotranspiration. This is a key parameter that controls the amount of water able to enter or leave the soil.

The increase in soil suction during dry periods, associated with de-saturation of the soil, is likely to cause a reduction of permeability in the intact material. However, tension or desiccation cracks in shallow layers are often observed during such periods, which contribute to the increase of global soil permeability. This duality of soil permeability is captured in ICFEP with a permeability model depicted in Fig. 18 (Potts and Zdravkovic, 1999).

The reduction of permeability from the saturated state, k_{sat}, to a minimum value, $k_{\min}$, is linked to the magnitude of suction, s, in Fig. 18a. An alternative variable for the horizontal axis is the degree of saturation, S_r, using the following relationship:

$$k = k_{sat} \cdot \Theta^{\frac{1}{2}} \cdot \left[1 - \left(1 - \Theta^{\frac{1}{m}} \right)^{m} \right]^{2} \quad (5)$$

where m is a fitting parameter, and Θ is a parameter dependent on the long-term degree of saturation, $S_{r,LT}$.

Conversely, the abrupt increase in permeability, to a maximum value, $k_{\max}$, due to desiccation cracking is linked to the occurrence of tensile principal total stresses, as depicted in Fig. 18b.

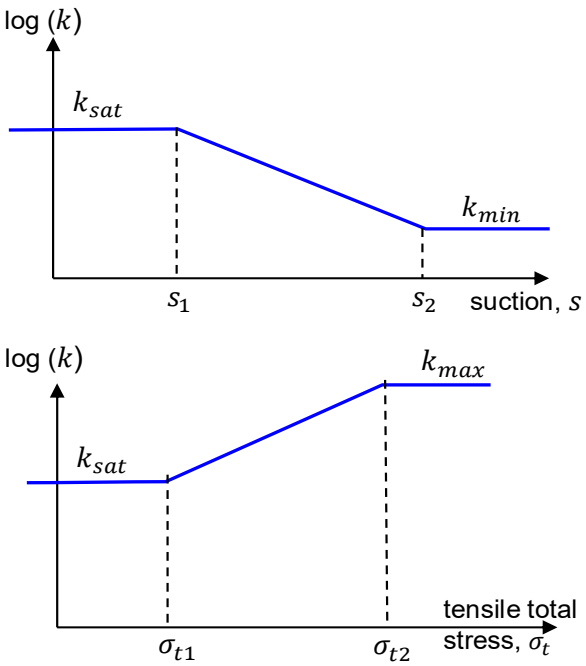

Figure 18. Permeability model as a function of (a) suction and (b) tensile total stress

3.3 Mechanical and SWR models

The formulation of the governing FE equations for unsaturated soils, as developed in ICFEP, is summarised in Smith (2003), Tsiampousi et al. (2017a, b) and Zdravkovic et al. (2018). The constitutive models of Georgiadis et al. (2005) and Tsiampousi et al. (2013b) are available in ICFEP for simulating the behaviour of moderately-expansive unsaturated soils and represent a modification and generalisation of the Barcelona Basic Model (BBM) of Alonso et al. (1990). The model, IC SSM (Imperial College Single Structure Model), adopts the standard concept of a single-porosity structure valid for most geomaterials.

Apart from a standard non-hysteretic soil-water retention (SWR) model of Van Genuchten (1980), a three-dimensional (3D) hysteretic SWR model of Tsiampousi et al. (2013a) is also available in ICFEP. Although the SWR curve may be plotted in terms of the volumetric water content, for consistency with the constitutive model it is defined in terms of the degree of saturation, S_r, taking account of its variation with both the suction, s, and the specific volume, v. As such, the SWR model is linked with the IC SSM constitutive model via the degree of saturation, S_r.

3.4 Life-cycle assessment

One of the difficulties in creating a numerical model of an existing earth embankment is establishing the current stress states in the embankment body and in the foundation soil. Many infrastructure embankments in the UK were constructed in the late 19th century without any records of construction and compaction of the clay. The vegetation growth in subsequent years and seasonal variations in rainfall and evapotranspiration have had a significant effect on the development of stress and pore pressure fields within the embankment. In order to examine the embankment's response to extreme events, it is important to establish a reasonably realistic water balance in the embankment, as it has been recognised that the ground response to rainfall depends on antecedent conditions.

Studying infrastructure slopes, Tsiampousi et al. (2017c) established a methodology for initialising the stress and pore pressure fields in slopes excavated in stiff overconsolidated clays. A similar methodology is applied in the study of earth embankments (Guo, 2020). To demonstrate the validity of the modelling process, a railway embankment in Essex, UK, is considered here as it was instrumented and monitored for a period of time (Ridley, 2010; Smethurst et al., 2015), thus enabling the numerical model to be verified against field measurements. A schematic picture of the embankment in Fig. 19 shows a cross-section containing a typical clay fill constructed on top of the natural London clay and topped by ash and ballast over the period of its life, in order to maintain the track elevation. The embankment is over 100 years old and it was monitored for a year from March 2006, in order to enable the assessment of the 'current' embankment state before the trees were

felled in March 2007. Monitoring then continued for another four years.

The mechanical behaviour of the clay fill was modelled with the constitutive model of Tsiampousi et al. (2013b) for unsaturated soils, while the permeability was simulated with a hydraulic model depicted in Fig. 18. Calibration and derivation of model parameters are given in Guo (2020).

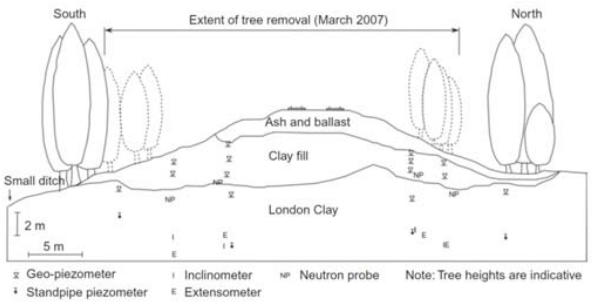

Figure 19. Cross section through a rail embankment (after Smethurst et al., 2015)

The FE analysis was initialised with a flat ground surface covered by grass, while FE elements of the fill were deactivated. The objective of this first stage was to establish the pore water pressure and stress conditions in the foundation soil, which reflect the effect of precipitation and evapotranspiration. As this is a generic stage, average long-term monthly rainfall data were incorporated in the analysis (Fig. 20). These were obtained from a weather station near the site, for a period of 30 years (1971 to 2000). Potential evapotranspiration is more difficult to quantify and exhibits small annual variations. The rates from April 2008 to March 2009, calculated with the FAO Penman-Monteith method (Allen et al. 1998) for deciduous trees with 2 m root depth, were applied in the analysis and are also shown in Fig. 20.

Both precipitation and evapotranspiration rates were applied monthly and a typical year was repeated 5 times (year 1 to 5), assuming grass cover on the flat ground surface. To account for the much smaller root depth (assumed to be 0.1 m) only 10% of the average monthly evapotranspiration rate in Fig. 20 was applied. The cycling of such hydraulic boundary conditions was ceased when the pore water pressure regime became stable. (i.e. after 5 years) The embankment was then constructed in year 6 and a grass cover was allowed to develop on the slope in years 7 to 10, applying the same hydraulic boundary conditions (precipitation and evapotranspiration) as in the first 5 years. For years 11 to 15 the latter boundary condition increased the rates to 50% of the average monthly rates shown in Fig. 20, representing the growth of shrubs with assumed 0.5 m root depth. Finally, in years 16 to 26 the growth of trees on embankment slopes was simulated by applying full average monthly evapotranspiration rates. The average monthly precipitation rates from Fig. 20 were applied throughout the 26 years.

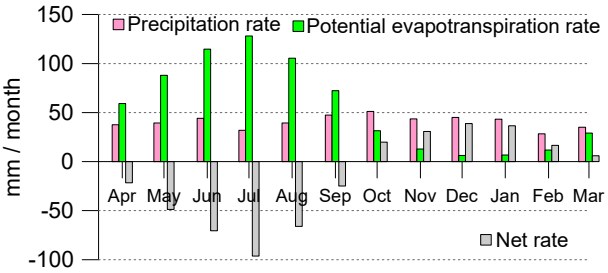

Figure 20. Precipitation and evapotranspiration for a typical year (after Tsiampousi et al., 2017c)

The end of this modelling process established the 'current' state of the embankment before vegetation removal. The predicted ground movements in the slope are compared with measurements taken over the one year before the removal of trees (March 2006 to March 2007, Fig. 21). Two monitoring points are located in the clay fill and two in the foundation soil, as shown in the inset of Fig. 21. The agreement is very satisfactory, indicating that the developed numerical model and the procedure to initialise the stress and pore pressure fields in the embankment are robust and accurate. The results clearly show seasonal effects in the embankment fill, with negative water balance in the summer months (i.e. higher evapotranspiration) causing shrinkage and large settlements, while replenishing water in winter months due to higher precipitation rates results in swelling of the clay and reduction of overall settlements. Fig. 22 shows snapshots of the contours of pore water pressures in the embankment and in the foundation soil in the summer (August) and in the following winter (March) of the monitored year. Consistent with the results in Fig. 21, they indicate that suctions (plotted as positive values) are high in the summer and reduce in the winter, with magnitudes broadly agreeing with in-situ measurements. Applying the strength reduction procedure of Potts & Zdravkovic (2012), as in the case of cut slopes in Section 2), the factor of safety of the embankment slope in March, just before the trees were removed, was calculated at 2.44.

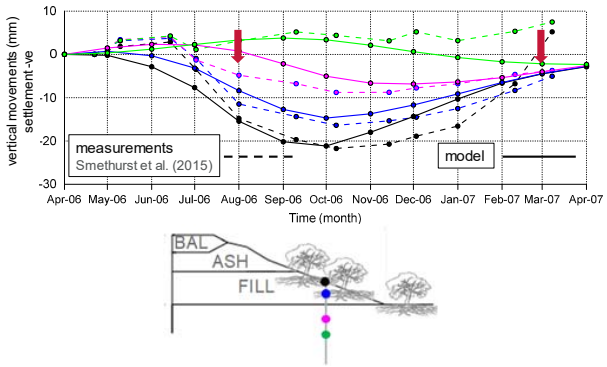

Figure 21. Predicted and measured vertical displacements before the removal of trees (after Guo, 2020)

The analysis was continued for a further 4 years, applying the same average monthly evapotranspiration rates as these do not change significantly, but applying the precipitation rates that were measured over that period, rather than generic rates used to establish the current state of the embankment. As the monitoring of the embankment continued for this period, it was possible to compare the predicted movements with measurements (Fig. 23), in the same cross-section depicted in the inset of Fig. 21.

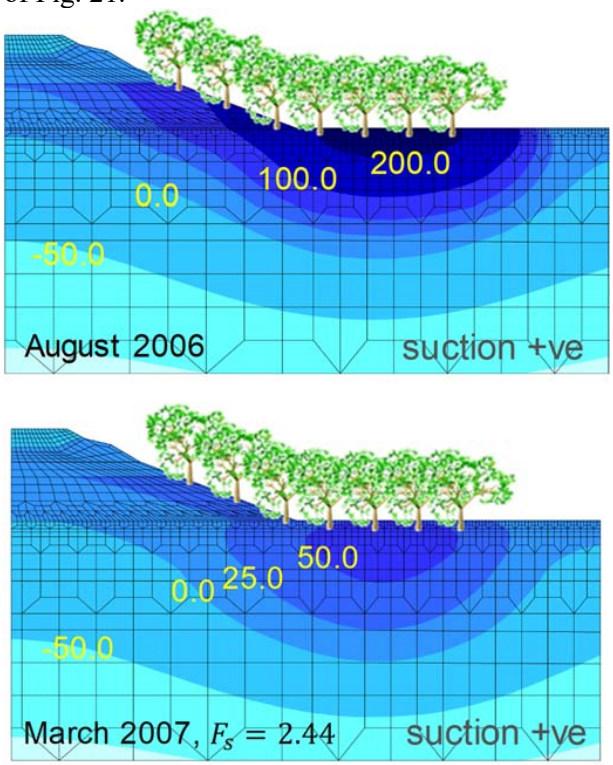

Figure 22. Predicted seasonal pore pressure variations (after Guo, 2020)

The results show significant heave in the clay fill, which is reasonably well captured by the numerical model. The foundation soil, however, does not appear to experience significant changes in displacements, which is also reproduced well by the model. The factor of safety in the embankment slope, calculated a year after the trees were removed (April 2008) was only 1.1, as suction in the clay fill were significantly depleted due to the lack of water uptake through the roots to contribute to evapotranspiration.

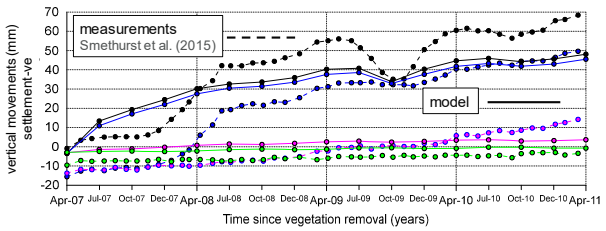

Figure 23. Predicted and measured vertical displacement after the removal of trees (after Guo, 2020)

4. CONCLUSIONS

The geotechnical problems selected for discussion in this paper demonstrate the need for increasing complexity of numerical tools to quantify serviceability and ultimate limit states and the risk posed by extreme conditions, to help streamline practical design guidance. Infrastructure monitoring is essential for providing field data that would build confidence in advanced numerical models and experience in using them. Equally, careful ground investigation and characterisation of soil behaviour are essential for deriving the appropriate input for constitutive modelling.

5. REFERENCES

Abbo, A.J., & Sloan, S.W. 1996. An automatic load stepping algorithm with error control. *Int. J. Num. Meth. In Eng*. 39: 1737-1759.

Alonso, E.E., Gens, A., & Josa, A. 1990. A constitutive model for partially saturated soils. *Géotechnique* 40 (3): 405-430.

Bazant, Z.P. & Jirasek, M. 2002. Nonlocal integral formulations of plasticity and damage: survey of progress. *Jnl. Eng. Mechanics* 128 (11): 1119-1149.

Brosse, A. 2012. *Study of the anisotropy of three British mudrocks using a hollow cylinder apparatus*. PhD thesis, Imperial College London.

Dounias, G.T., Potts, D.M. & Vaughan, P.R. 1996. Analysis of progressive failure and cracking in old British dams. *Géotechnique* 46 (4): 621-640.

Feddes, R.A., Kowalk, P.J., & Zaradny, H. 1978. *Simulation of field water use and crop yield*. John Wiley & Sons, New York.

Galavi, V. & Schweiger, H.F. 2010. Nonlocal multilaminate model for strain softening analysis. *Int. Jnl. Geomechanics* 10: 30-44.

Gasparre, A. 2005. *Advanced laboratory characterisation of London clay*. PhD thesis, Imperial College London.

Georgiadis, K., Potts, D.M., & Zdravkovic, L. 2005. Three-dimensional constitutive model for partially and fully saturated soils. *ASCE Int. J. Geomech*. 5 (3): 244-255.

Guo B.W.L. 2020. *Resilience and sustainability of flood defenses.* PhD thesis, Imperial College London.

Hight, D.W., McMillan, F., Powell, J.J., Jardine, R.J. & Allenou, C.P. 2003. *Some characteristics of London Clay*. Proc. Int. Workshop on characterization and engineering properties of natural soils, Singapore, Vol. 2:81-908.

Ho, X. 2019. *Assessment of serviceability and stability of sloped excavations in stiff clay*. MEng internal project. Imperial College London.

Hosseini Kamal, R. 2012. *Experimental study of the geotechnical properties of UK mudrocks*. PhD thesis, Imperial College London.

Hosseini Kamal, R., Coop, M.R., Jardine, R.J. & Brosse, A. 2014. The post-yield behavior of four Eocene-to-Jurassic UK stiff clays. *Géotechnique* 64 (8): 620-634.

Kovacevic, N. 1994. *Numerical analysis of rockfill dams, cut slopes and road embankments*. PhD thesis, Imperial College, University of London.

Kovacevic, N., Hight, D.W. & Potts, D.M. 2007. Predicting the stand-up time of temporary London Clay slopes at Terminal 5, Heathrow Airport. *Géotechnique* 47 (5): 953-982.

Potts, D.M., Dounias, G.T., & Vaughan, P.R. 1990. Finite element analysis of progressive failure of Carsington embankment. *Géotechnique* 40 (1): 79-101.

Potts, D.M., Kovacevic, N., & Vaughan, P.R. 1997. Delayed collapse of cut slopes in stiff clay. *Géotechnique* 47 (5): 953-982.

Potts, D.M, & Zdravkovic, L. 1999. *Finite element analysis in geotechnical engineering: theory*. Thomas Telford, London.

Potts, D.M, & Zdravkovic, L. 2001. *Finite element analysis in geotechnical engineering: application*. Thomas Telford, London.

Potts, D.M., & Zdravkovic, L. 2012. Accounting for partial material factors in numerical analysis. *Géotechnique* 62 (12): 1053-1065.

Sheng, D., & Sloan, S.W. 2001. Load stepping schemes for critical state models. *Int. J. Num. Meth. Eng*. 50: 67-93.

Smith, P.G.C. 2003. *Numerical analysis of infiltration into partially saturated soil slopes*. PhD thesis, Imperial College, University of London.

Smith, P.G.C., Potts, D.M., & Addenbrooke, T.I. 2008. A precipitation boundary condition for finite element analysis. In: *Unsaturated soils: Advances in geo-engineering*. Eds. Toll, D.G., Augarde, C.E., Gallipoli, D. & Wheeler, S.J. CRC Press: 773-778.

Summersgill, F.C. 2015. *Numerical modelling of stiff clay cut slopes with nonlocal strain regularisation*. PhD thesis, Imperial College London.

Summersgill, F.C., Kontoe S. & Potts, D.M. 2017. On the use of nonlocal regularisation in slope stability problems. *Computers and Geotechnics* 82: 187-200.

Taborda, D.M.G. & Zdravkovic, L. 2012. Application of a Hill-Climbing technique to the formulation of a new cyclic nonlinear elastic constitutive model. *Computers and Geotechnics* 43: 80-91.

Taborda, D.M.G., Potts, D.M. & Zdravković, L. 2016. On the assessment of energy dissipated through hysteresis in finite element analysis. *Computers and Geotechnics* 71: 180-194.

Tsiampousi, A., Zdravkovic, L., & Potts, D.M. 2013a. A three-dimensional hysteretic soil-water retention curve. *Géotechnique* 63 (2): 155-164.

Tsiampousi, A., Zdravkovic, L., & Potts, D.M. 2013b. A new Hvorslev surface for critical state type unsaturated and saturated constitutive models. *Computers and Geotechnics* 48: 156-166.

Tsiampousi, A., Smith, P.G.C., & Potts, D.M. 2017a., Coupled consolidation in unsaturated soils: An alternative approach to deriving the governing equations. *Computers and Geotechnics* 84: 238-255.

Tsiampousi, A., Smith, P.G.C., & Potts, D.M. 2017b., Coupled consolidation in unsaturated soils: From a conceptual model to applications in boundary value problems. *Computers and Geotechnics* 84: 256-277.

Tsimapousi, A., Zdravkovic, L., & Potts, D.M. 2017c. Numerical study of the effect of soil-

atmosphere interaction on the stability and serviceability of cut slopes in London clay. *Can. Geotech. J*. 54: 405-418.

Van Genuchten, M.T. 1980. A close-form equation for predicting the hydraulic conductivity of unsaturated soils. *Soil. Sci. Soc. Am. J*. 44: 892-898.

Vardulakis, I.G. & Sulem, J. 1995. *Bifurcation analysis in geomaterials*. Chapman & Hall, London.

Vaughan, P.R. 1994. Assumption, prediction and reality in geotechnical engineering. *Géotechnique* 44 (4): 573-609.

Vermeer, P.A. & Brinkgrave, R.B.J. 1994. A new effective non-local strain measure for softening plasticity. In *Localisation and bifurcation theory for soils and rocks*. Eds. Chambon, R., Desrues, J. & Vardoulakis, I.G., 89-100, Rotterdam, Balkema.

Walbancke, H.J. 1976. *Pore pressures in clay embankments and cuttings*. PhD thesis, Imperial College, University of London.

Zdravković, L., Tsiampousi, A. & Potts. D.M. 2018. On the modelling of soil-atmosphere interaction in cut and natural slopes. *7th Int. Conf. on Unsaturated Soils* UNSAT 2018. Eds. Ng, C.W.W., Leung, A.K., Chiu, A,C.F. & Zhou, C. HKUST, Hong Kong.

Zdravković, L., Potts, D.M. & Taborda, D.M.G. 2019. Integrating laboratory and field testing into advanced geotechnical design. 7th Int. Sym. on Deformation Characteristics of Geomaterials, IS-Glasgow 2019, Eds. Tarantino, A. & Ibraim, E. EDP Sciences.

Zervos, A., Papanastasiou, P. & Vardoulakis, I. 2001. Finite element displacement formulation for gradient elastoplasticity. Int. Jnl. Numer. Meth. Engineering 50 (6): 1369-1388.